The ECCO 1° global WOCE Synthesis: Mass and Property Transports

D. Stammer and C. Wunsch for the ECCO Consortium.

Scripps Institution of Oceanography and Massachusetts Institute of Technology

Summary

Rigorous global ocean state estimation methods are required to produce dynamically consistent model/data syntheses from which time-varying ocean transport of heat, freshwater and momentum can be computed, as well as their regional divergence.

All results shown below are quantities that can not directly be observed: ocean state estimation is important for obtaining estimates of all climate relevant observable and unobservable time-dependent fields. Those include the flow field, transports, mixed layer depths, overturning, and especially the surface heat, freshwater and momentum fluxes that are consistent with ocean observations.

Methodology

The ECCO global WOCE synthesis is used here to analyze ocean volume, heat and freshwater transports. Time-mean horizontal transports, estimated from this fully time-dependent constrained circulation, are now generally consistent with the time-independent inverse estimates from box inversions, with especially good agrement in the southern hemisphere. Dynamically consistent variations in the model show temporal variability of oceanic heat transports, heat storage and atmospheric exchanges that are complex and show a strong dependence upon location, depth, and time-scale. One can now study the dynamics of both the mean and time variability from the model with the reassurance that it is consistent with the bulk of the WOCE observations.
We use results from the global WOCE synthesis on a 1° global grid ($\pm$ 80°) and over the 10-year period 1992-2001. Those results are obtained by constraining the MIT ocean circulation model by the bulk of the WOCE data set, including altimetry, SST, SSS, scatterometry, XBT, PALACE and ARGE profiles, hydrographic sections, and drifter velocities.

The synthesis is obtained by forcing the model to consistency, within a complex, specified error margin, with those fields by using the model adjoint (Marotzke et al., 1999) to modify the initial temperature and salinity conditions over the full water column and to adjust the time-varying meteorological forcing fields over the full estimation period.

Volume Transports

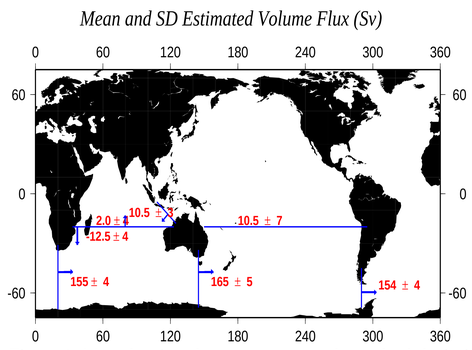

Figure 1: Map showing the mean mean and standard deviation of volume flux in open loops of the world ocean. The estimated mean circulation around Australia involves a net volume transport of 10.5 Sv through the Indonesian Throughflow and the Mozambique Channel. This flow regime exists on all time scales longer than one month—rendering the variability in the South Pacific strongly coupled to that in the Indian Ocean. The volume transport between Mozambique and Australia shows 2 Sv going norward, in contrast to recent box inversions that require 4 Sv going southward. We note that the estimates of the circulation around Australia of about 10 Sv and the ACC transpor of about 155 Sv has converged with previous findings in both aspects, e.g., from Ganachaud and Wunsch (2000).

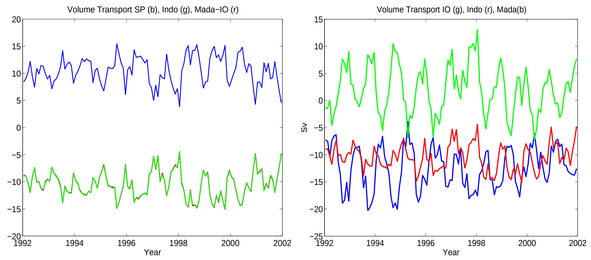

Figure 2: (Left Panel): Volume flux plotted separately for the South Pacific and the Indonesian Throughflow/ Indian Ocean (negative). All three curves essentially track each other but with opposite signe.

(Right Panel): Volume transports, plotted separately for the Indonesian Throughflow (red), the Madagascar Channel (blue) and the Indian Ocean between Madagascar and Australia (green).

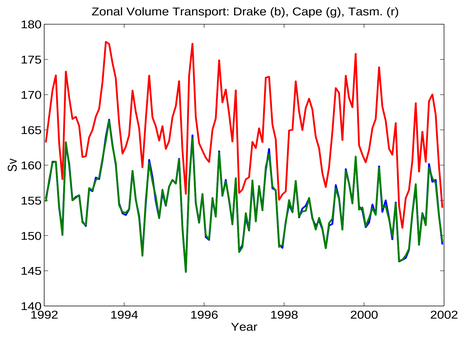

Figure 3: Antarctic Circumpolar Current volume transports, plotted separately for sections sourth of Africa (green), Drake Passage (blue) and south of Tasmania (red). Note the decrease in ACC transport during the 10-year period by about 5 Sv.

Mean Heat and Freshwater Transports

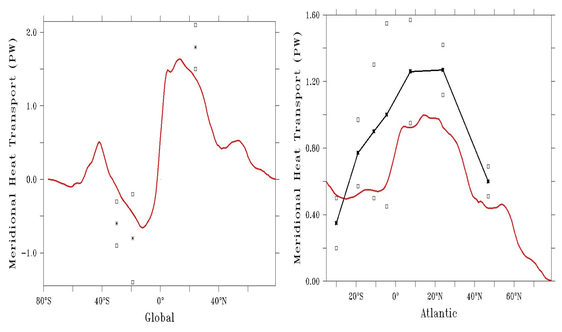

Figure 4: Time-mean meridional heat transport, zonally integrated over the entire ocean (left) and for just the Atlantic sector (right). Also shown are Ganachaud and Wunsch results from a box inversion and their error bars.

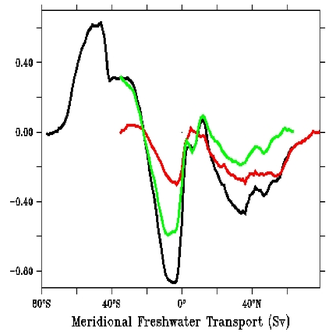

Figure 5: Zonally integrated meridional freshwater transport for the global ocean (black), the Atlantic (red) and the Indo-Pacific (green).

Time-varying Heat Transports

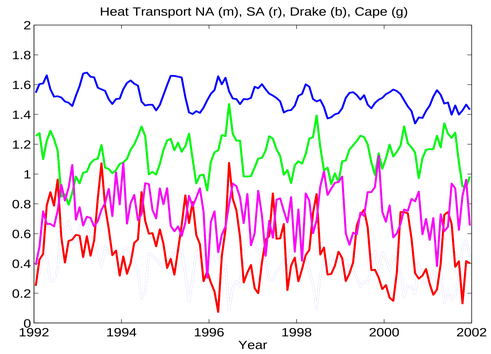

Figure 6: Heat transports through the Drake Passage (blue) and south of Africa (green). Also shown are northward heat transports in the South Atlantic across 30° S (red) and the North Atlantic across 30° N (magenta). Note the difference of about 0.5 PW between the transport through Drake Passage and south of Africa that enters the Atlantic via the "cold route". Note also the decrease in heat transport through Drake Passage and into the South Atlantic by about 0.1 PW during the 10-year period.

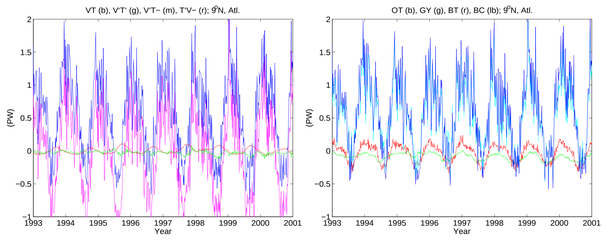

Figure 7: (left) Timeseries $H_Q(t) = \int\int v\theta dzdx$ (blue curves) across 9° N in the Atlantic Ocean. Also shown are $\int\int v'\theta' dzdx$, $\int\int \overline{\theta} v' dzdx$ and $\int\int \overline{v}\theta' dzdx$ as green, magenta and red lines, respectively. (right) Temperature transport time series evaluated as contributions from the overturning (OT; blue), the gyre (GY; green), the vertical average (BT, red) and baroclinic circulation (BC, light blue), respectively. (This figures shows actually results from an earlier optimization on a 2° horizontal gris (*Stammer et al.*, 2002a,b).)

Regional Heat Budgets

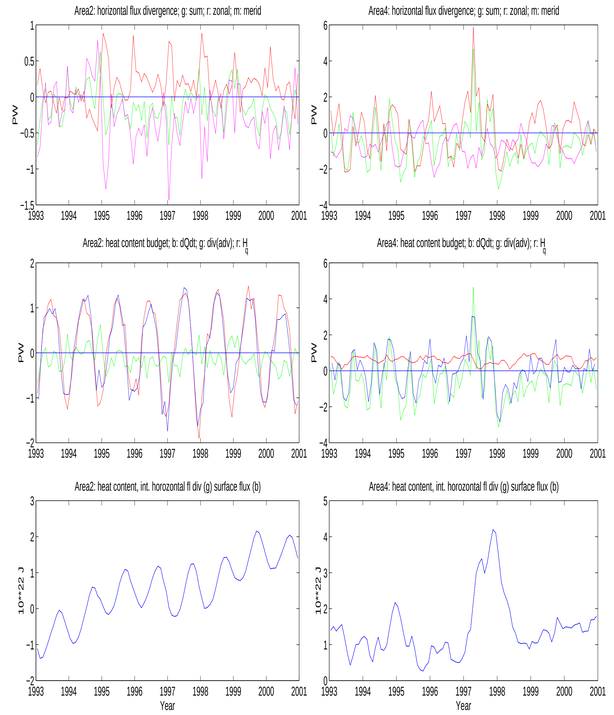

(top) Horizontal temperature flux convergence in two regions, one centered at 30° N and covers the Pacific east of 180° E. The second region represents $\pm$ 10° latitude, 230° to 280° E. Plotted separately in the top panel plotted are contributions for the zonal (red), the meridional horizontal (magenta) transport divergences and the net convergence (green). (middle) Horizontal temperature flux convergence (green), net surface heat flux (red) and time-rate of change of heat content in the region (blue). (bottom) Timeseries of heat content (blue). (This figures shows actually results from an earlier optimization on a 2° horizontal gris (*Stammer et al.*, 2002a,b).)

References

[1] Marotzke, J., R. Giering, Q. K. Zhang, D. Stammer, C. N. Hill, and T. Lee, 1999: Construction of the adjoint MIT ocean general circulation model and application to Atlantic heat transport sensitivity, J. Geophys. Research, 104, 29,529 - 29,548, 1999.

[2] Stammer, D., C. Wunsch, R. Giering, C. Eckert, P. Heimbach, J. Marotzke, A. Adcroft, C.N. Hill, and J. Marshall, 2002, The global ocean circulation during 1992 –1997, estimated from ocean observations and a general circulation model, *J. Geophys. Res.*, 107, C9.

[3] Stammer, D., C. Wunsch, R. Giering, C. Eckert, P. Heimbach, J. Marotzke, A. Adcroft, C.N. Hill, and J. Marshall, 2002: Volume, Heat and Freshwater Transports of the Global Ocean Circulation 1993 –2000, Estimated from a General Circulation Model Constrained by WOCE Data, *J. Geophys. Res.*, in press.

November 15, 2002